RESEARCH ARTICLE

Persistent free radicals in humin under redox conditions and their impact in transforming polycyclic aromatic hydrocarbons

Hanzhong Jia[1,2], Yafang Shi[1], Xiaofeng Nie[1], Song Zhao[1], Tiecheng Wang (✉)[1], Virender K. Sharma (✉)[3]

1 College of Resources and Environment, Northwest A&F University, Yangling 712100, China
2 State Key Laboratory of Soil Erosion and Dryland Farming on Loess Plateau, Institute of Soil and Water Conservation, Northwest A&F University, Yangling 712100, China
3 Program for the Environment and Sustainability, Department of Occupational and Environmental Health, School of Public Health, Texas A&M University, College Station, TX 77843, USA

HIGHLIGHTS

- Regulation of redox conditions promotes the generation of free radicals on HM.
- HM-PFRs can be fractionated into active and inactive types depending on stability.
- The newly produced PFRs readily release electrons to oxygen and generate ROS.
- PFR-induced ROS mediate the transformation of organic contaminants adsorbed on HM.

GRAPHIC ABSTRACT
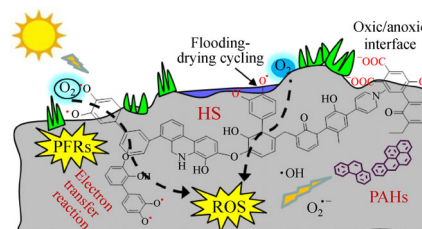
ABSTRACT

The role of humic substance-associated persistent free radicals (PFRs) in the fate of organic contaminants under various redox conditions remains unknown. This study examined the characterization of original metal-free peat humin (HM), and HM treated with varying concentrations of H_2O_2 and L-ascorbic acid (VC) (assigned as H_2O_2-HM and VC-HM). The concentration of PFRs in HM increased with the addition of VC/H_2O_2 at concentrations less than 0.08 mol/L. The evolution of PFRs in HM under different environmental conditions (e.g., oxic/anoxic and humidity) was investigated. Two types of PFRs were detected in HM: a relatively stable radical existed in the original sample, and the other type, which was generated by redox treatments, was relatively unstable. The spin densities of VC/H_2O_2-HM readily returned to the original value under relatively high humidity and oxic conditions. During this process, the HM-associated "unstable" free radicals released an electron to O_2, inducing the formation of reactive oxygen species (ROS, i.e., $^\bullet OH$ and $^\bullet O_2^-$). The generated ROS promoted the degradation of polycyclic aromatic hydrocarbons based on the radical quenching measurements. The transformation rates followed the order naphthalene>phenanthrene>anthracene>benzo[a]pyrene. Our results provide valuable insight into the HM-induced transformation of organic contaminants under natural conditions.

1 Introduction

Humic substances (HSs) contain significant quantities of free radicals, which have been detected by the electron paramagnetic resonance (EPR) technique (Rex, 1960; Saab and Martin-Neto, 2004). Free radicals in HSs may originate from humification of plant tissues via chemical and biological processes (Munk et al., 2015). During these processes, hydrolytic and dehydrogenative reactions induce the generation of semiquinone units with free radicals, possibly conjugated to aromatic polymers (Rex, 1960). Consequently, a large amount of free radicals may be retained on the semiquinone units within the HS matrix

✉ Corresponding authors
E-mail: wangtiecheng2008@126.com (T. Wang); vsharma@tamu.edu (V. Sharma)

(Saab and Martin-Neto, 2004). These free radicals are either trapped by the polymeric network or stabilized in the π-electron system in HSs, promoting their persistence, and thus, have been named environmentally persistent free radicals (EPFRs) (Vejerano et al., 2018; Kaikai et al., 2019).

The EPR characteristics related to their structure, reactivity, and physicochemical properties are crucial parameters of HSs (Roden et al., 2010). For instance, EPFR type and concentration may be used to assess the humification degree of HSs in soil (Simpson, 2002). Free organic radicals readily induce charge transfer complexes with hydrophobic organic compounds, which are involved in the radical-driven interaction of pesticides with HSs (Piccolo et al., 1998). The charge transfer process may also result in polymerization and redox reactions of HSs with organic compounds. For instance, electron transfers from persistent radicals could oxidize carbamate and organochlorine in soil (Cwielag-Piasecka et al., 2017). Overall, EPFRs may be related to the interactions of HSs with other organic compounds, and subsequently additional redox reactions and transformation processes.

The characteristics of HS-associated EPFRs depend not only on the origin of material but also on environmental factors such as transition metals, light irradiation, and redox conditions. Many investigations have been conducted on the photolytic processes in natural phases. HSs have photosensitization due to the high degree of humification and polymeric phenolic moieties in their structure (Li et al., 2016). During photo-irradiation of HSs, electron transfer from the photosensitized radical species to the oxygen molecule promotes the generation of reactive oxygen species (ROS) (Tian et al., 2019). Electrochemically reduced HSs, which contain redox-active moieties, have the ability to transfer electrons to O_2, which induces the formation of $\cdot OH$ without light irradiation (Page et al., 2012). The formed ROS may attack pollutants in aquatic/ soil environments and initiate their degradation. The variation of redox conditions at oxic/anoxic interfaces and flooding-drying cycling processes may induce either oxidation or reduction of HS (Jin et al., 2019). Intermediate radicals might also be produced in the HS matrix during these processes. Significantly, the literature has limited information on the evolution and decay of HS-associated EPFRs and their correlations with ROS formation.

Among three HS fractions (humin (HM), fulvic acid (FA), and humic acid (HA)), HM is recognized as the predominant soil fraction possessing free organic radicals (Saab and Martin-Neto, 2004). However, most of the previous redox reaction studies of HSs involved soluble HSs and their quinoid analogs, while only few investigations have been conducted using solid forms of HSs (i.e., HM) (Roden et al., 2010). We have therefore chosen HM as the representative HS in our study. In this study, HM was extracted from a peat soil, which has typically been applied as a soil model for determining the role of HSs in

the fate of contaminants (Cwielag-Piasecka et al., 2017). Polycyclic aromatic hydrocarbons (PAHs), a class of typically hydrophobic contaminants, are widely detected in soil and readily interact with HM fractions (Jia et al., 2016). In this study, we selected PAHs as the representative contaminants to gain insight on the electron-transfer reactions that may occur during the interactions between HSs and PAHs. We hypothesized that the EPFR properties of HM may influence the redox reactions to generate ROS and subsequently induce the transformation of PAHs. To test this hypothesis, metal-free HM was exposed to different redox conditions that may be encountered in the natural environment to elucidate the influence of varied free radicals in HSs on the transformation of the selected contaminants. The objectives of the present research were to (i) evaluate the properties of free organic radicals in HM under various redox conditions, (ii) investigate the effect of the type and concentration of PFRs on the formation of ROS, and (iii) comprehend the role of HM as the redox mediator in transforming PAHs. The obtained results shed light on the impacts of redox conditions on the evolution of PFRs, which may have a potential impact on the transformation of organic contaminants in natural environments.

2   Materials and methods

2.1   Chemicals and materials

Details of the chemicals used are provided in Text S1. Metal-free HM in peat soil was separated by a protocol from the International Humic Substances Society (IHSS) and details are given in Text S2.

2.2   Preparation of oxidized/reduced HM

In this investigation, humin was exposed to H_2O_2 and ascorbic acid, similar to a previous study by Oniki and Takahama (1994). To prepare HM samples at different extents of oxidation, 1.0 g of the separated sample was mixed with 20 mL of H_2O_2 at concentrations of 0.01, 0.02, 0.04, 0.08, and 0.10 mol/L. The mixtures were vigorously stirred for 24 h at room temperature. As investigated previously, the change in EPR characteristics of HM occurred within the first 4.0 h during the treatment and no further change was seen after 24 h (Oniki and Takahama, 1994). Details of preparation of oxidized/reduced HM are provided in Text S3.

2.3   Characterization of HM samples

The elemental compositions (i.e., C, H, N, and S) of samples were analyzed with a Pekin-Elmer 2400 SERIES II analyzer (Waltham, Massachusetts, USA). Oxygen content was calculated by the mass difference. Ash content

of HM samples was determined after combustion at 800°C for 4 h. X-ray photoelectron spectroscopy was conducted using an ESCA-Laboratory-250i-Xi spectrometer (Shimadzu Co., Kyoto, Japan), which consisted of monochromatic Al Kα radiation (180 W, 12 mA, 15 kV) and a diameter beam spot of 500 mm.

2.4 Stability of the HS-associated free radicals

In the experimental set-up of oxic conditions in various relative humid (RH) environments, HM samples were in brownish desiccators. The humidity of 7%, 60%, and 100% in the desiccators was controlled by silica gel (self-indicator), saturated NaBr solution, and H_2O, respectively. For the experiments without O_2 (anoxic conditions) and humidity (no water), the HM samples were transferred into an anoxic chamber. At pre-selected intervals of different days (0 d, 1 d, 3 d, 6 d, and 30 d), the samples under various conditions were analyzed immediately by the EPR technique. The detailed instrument and operating parameters are provided in Text S4.

2.5 PAHs transformation

PAHs, including benzo[a]pyrene (B[a]P), anthracene (ANT), phenanthrene (PHE), and naphthalene (NAP), were used as the model molecules to probe the potential transformation ability of organic contaminants by metal-free HM samples. PAH-spiked HM samples were initially prepared by adopting a protocol from our previous study (Jia et al., 2012). Instrument details are provided in Text S5. The concentration of PAHs was quantified by a Thermo Fisher Ultra 3000 HPLC (Waltham, Massachusetts, United States). The extraction efficiencies of the freshly prepared PAH-spiked HM samples were higher than 95% (Table S1). This indicated that the adsorption of PAHs on HM had no significant impact on the extraction procedure. To determine the role of ROS, degradation of

PAHs was performed in the presence of benzoquinone (p-BQ) and coumarin, which individually function as the $^{\bullet}O_2^-$ and $^{\bullet}OH$ scavengers, respectively. The contents of p-BQ and coumarin in HM samples were 0.16 mg/g and 0.12 mg/g, respectively (Jia et al., 2015). To further investigate the potential generation of ROS, the spin-trapping EPR technique was applied in suspension of the original or treated HM samples (H_2O_2-HM and VC-HM). Detailed information for the spin trapping experiment and EPR measurements is given in Text S6.

3 Results and discussion

3.1 Characterization of HM samples

Initially, the presence of free radicals on original peat HM was explored by EPR. The EPR spectrum in Fig. 1(a) presents a single and unstructured signal with a g-factor of ~2.0026 and peak-to-peak distance (ΔH_{p-p}) ranging from 4 to 6 G. This is a typical characteristic of free organic radicals in natural organic matter obtained from soil, sediment, and aquatic phases (Oniki and Takahama, 1994). According to the g-factor values, these free organic radicals are assigned as carbon-centered "aromatic" radicals, probably located at the condensation subsystems of aromatic rings (Jia et al., 2016). Comparably, the g-factors of dissolved organic matters (DOMs) (e.g., fulvic acid and humic acids), are in the range of 2.0035−2.0050, which include "oxygen-centered" radicals such as quinone, semiquinone, or even aromatic substituted semiquinone-type radicals (Saab and Martin-Neto, 2004). The concentration of free radicals in peat HM is ~5 × 10^{17} spins/g. Previous studies have reported spin concentrations of the free organic radicals in soil samples varying from ~0.5 × 10^{17} to 1 × 10^{18} spins/g, which could be attributed to their complex molecular structures, different biomass sources, and numerous humification processes (Oniki and
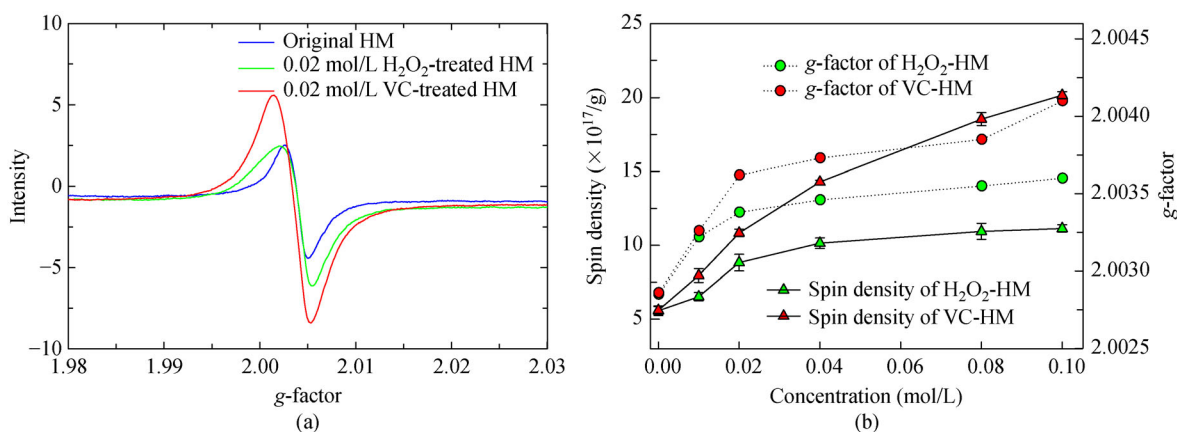

Fig. 1 (a) EPR spectra of the isolated peat humins (HM) (or original HM), and H_2O_2 and L-ascorbic acid (VC) treated HM samples, assigned as H_2O_2-HM and VC-HM samples, respectively; (b) Variation of peak area and g-factor for the treated HM by H_2O_2 and L-ascorbic acid (VC) at varied concentrations ranging from 0.0 to 0.10 mol/L.

Takahama, 1994; Saab and Martin-Neto, 2004). The spin density of peat HM is relatively higher than that of DOM extracted from aquatic phases (Paul et al., 2006). This may be attributed to the fact that HM has higher amounts of aromatic carbons and more electron-conjugated systems compared to aquatic DOM, which facilitates the stabilization of free radicals (Saab and Martin-Neto, 2004). The molecular weight of peat HM is $\sim 1 \times 10^6$ Da (Simpson, 2002), which gives one radical per three molecules of HM.

In this study, the variation in spin densities of treated HM samples was examined. As shown in Fig. 1b, the spin density of the initial EPR signal increased with an increase in the amount of H_2O_2 added; treatment by H_2O_2 produced a gradual increase in spin densities from $\sim 5.5 \times 10^{17}$ to $\sim 10 \times 10^{17}$ spins/g when the concentration of H_2O_2 was lower than 0.04 mol/L. However, limited increase of spin density was observed with further increase in H_2O_2 concentration. Increase in both g-factor and spin density may be due to an increase of the additional oxygen content (carbonyl C = O groups) and/or an unpaired electron shifting to an oxygen atom via spin-orbital interaction with oxygen-containing functional groups. A previous study has also reported that exposure to O_2 or treatment by oxidative agents resulted in an increase in free radicals from the content present in the original samples (Maskos et al., 2005).

The evolution of spin density of the VC-HM samples (i.e., under redox conditions) at various concentrations of VC from 0.01 to 0.10 mol/L was monitored (Fig. 1b). A similar tendency was observed for the VC-HM sample; the spin densities gradually increased with increasing addition of VC, followed by no further change. In general, the change in spin density correlated well with the degree of reduction, which was in agreement with a previous study by Oniki and Takahama (1994). The reducing agent treatments induced an increase in g-factor from 2.0026 to ~ 2.0038, indicating that the newly formed free organic radicals included more oxygen-centered free radicals. In addition, the value of ΔH_{p-p} increased from 5.5 to ~ 9.0 (G) after treatment by 0.02 mol/L H_2O_2/VC (Fig. 1(a)), suggesting the generation of different types of free organic radicals. Previous studies generally found an increase in the spin concentration when HM was treated with a reductant (Senesi et al., 1977; Oniki and Takahama, 1994). For example, the treatment of Ando HM by a dithionite ion caused an increase in spin concentrations, reaching a maximum value of $\sim 18 \times 10^{17}$ spins/g from 9.7×10^{17} spins/g (Oniki and Takahama, 1994). Similarly, the spin concentrations of fulvic materials from Canada Podzol markedly increased to 30.7×10^{17} spins/g, which was an increase of 67 times over that prior to addition of $NaBH_4$. When the same sample was reduced by $SnCl_2$, the concentrations of free radicals increased by 108 times (Senesi et al., 1977). The increases in spin densities are significantly influenced by the physicochemical properties of HS and/or differences in the reaction conditions, such as pH and type and concentration of reductive agents.

Next, the functional groups on the surfaces of the treated HM samples were monitored (Table S2). In the H_2O_2-HM sample, the oxygen content (O/C) at the surface of HM increased, whereas the hydrogen content decreased. The surface O/C of HM increased from 0.65 to 0.78 after oxidation with 0.10 mol/L H_2O_2. Comparatively, the VC-HM sample had a slightly decreased O/C value of 0.56 (Table S2). The reduction resulted in a loss of O functionalities relative to the original HM, indicated by the decrease in the C/H ratio from 7.67 (HM) to 6.09 (VC-HM) (Table S2). These results revealed that the reductive treatment (or VC-HM sample) decreased the surface polarity ((O + N)/C) of the HM. In the case of the oxidative treatment (or H_2O_2-HM sample), the surface polarity increased. As shown in Fig. 1, both reductive and oxidative treatments increased the spin densities of HM samples. The spin densities of free radicals had no correlation with the surface polarities (Fig. S2).

As shown in Fig. 2 and Table S2, the surface carbon components of the original HM sample accounted for 36.4%, 18.0%, and 7.6% of C-C, C-O, and C = O groups, respectively. The H_2O_2-HM sample had an increased percentage of the carbon component of C = O (Table S2). In the 0.10 mol/L VC-HM sample, the reduction process showed a 5.1% decrease in the carbon component of C = O group. The oxidative/reductive treatments of HM insignificantly influenced the content of aromatic C-C groups. The reductive and oxidative treatments of HM increased the amount of carbon components in the C-O groups. The obtained results suggested that the redox reactions promoted the formation of quinone-type and phenolic OH moieties in HM samples.

3.2 Fate of free organic radicals under various conditions

The newly produced EPFRs may exhibit a different evolution and fate from the original free radicals under natural conditions. The original and treated samples were exposed to different oxygen and humidity conditions to investigate the potential stability of HM-associated free organic radicals. An evolution of radical concentration was monitored for more than one month. The spin densities of the original HM sample were relatively constant during the aging period under natural ambience at RH = 60% (Fig. 3(a)). However, the concentrations of free organic radicals of the treated HM samples gradually decreased with increasing aging time. After 15 d, the spin densities of H_2O_2-HM and VC-HM decreased to a relatively constant value of $\sim 6 \times 10^{17}$ spins/g, which was equivalent to the amount of free radicals in the original HM. The decays of EPFRs in H_2O_2-HM and VC-HM samples are depicted as a function of the reaction time (Fig. S3), similar to a previous study by Jia et al. (2016). The free organic radicals in H_2O_2-HM and VC-HM samples exhibited similar decay trends with a 1/e lifetime of ~ 17 d.

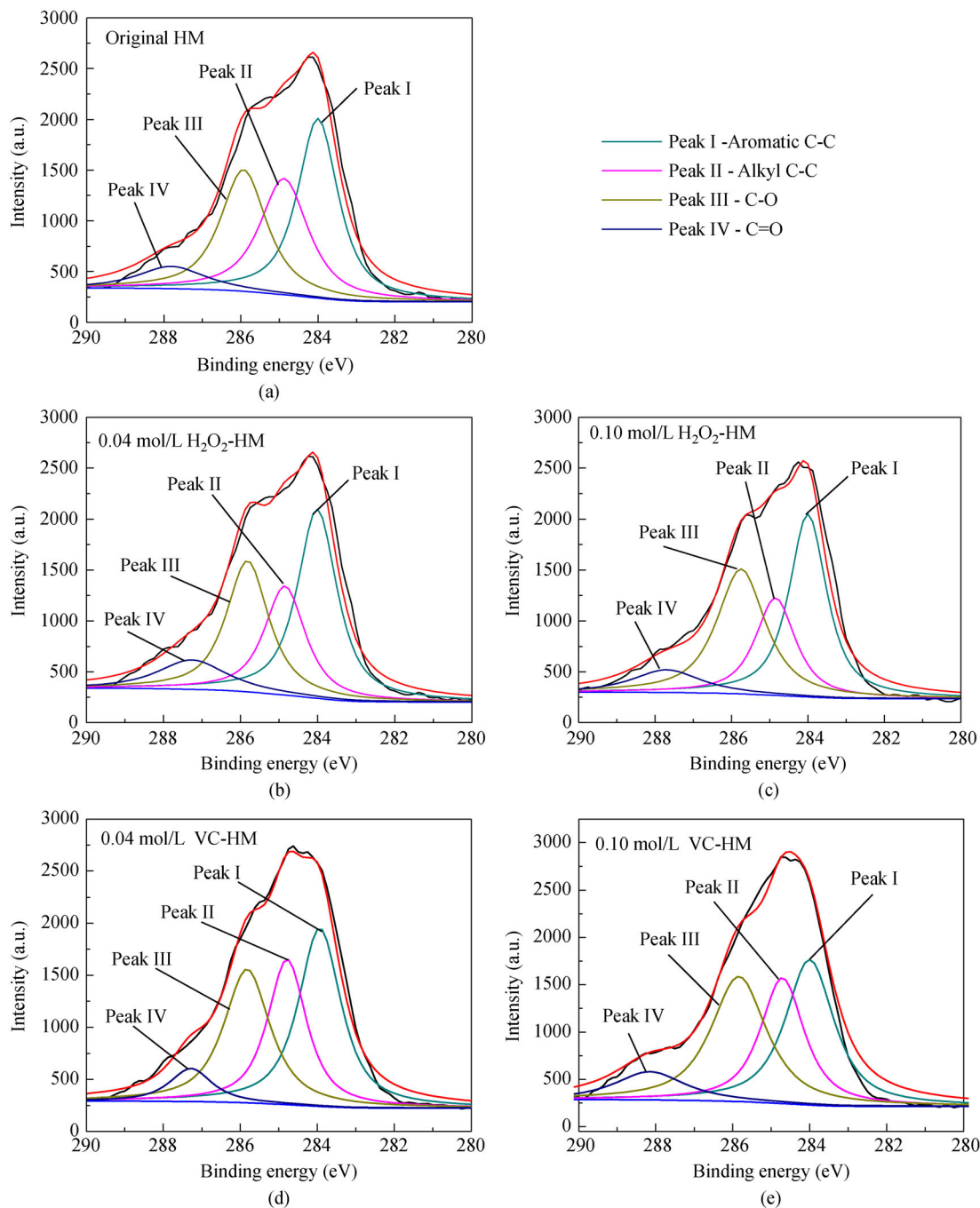At a RH of 7%, two time periods of spin density

Fig. 2   X-ray photoelectron spectra (XPS) of the original and treated peat HM, including (a) original HM (or untreated samples), (b) HM treated with 0.04 mol/L H$_2$O$_2$, (c) HM treated with 0.10 mol/L H$_2$O$_2$, (d) HM treated with 0.04 mol/L L-ascorbic acid, and (e) HM treated with 0.10 mol/L L-ascorbic acid.

evolution appeared, i.e., a slight increase followed by a gradual decay (Fig. 3(b)). The initial increase of radical concentrations could be attributed to the formation of secondary radicals upon exposure to air (Maskos et al., 2005). Carbohydrates on tobacco were readily decomposed to form aromatic molecular precursors such as catechol and other phenolic compounds (Maskos et al., 2005). These hydroquinone/catechol-type species did not

initially produce free organic radicals. After exposure to air, however, these precursors were readily converted to persistent radicals such as semiquinone-type radicals, accompanied by the increased spin densities and g-values with increasing aging time (Maskos et al., 2005). Similarly, the treatment of HM samples under reductive conditions also induced the generation of phenolic moieties, which may be subsequently converted to free organic radicals
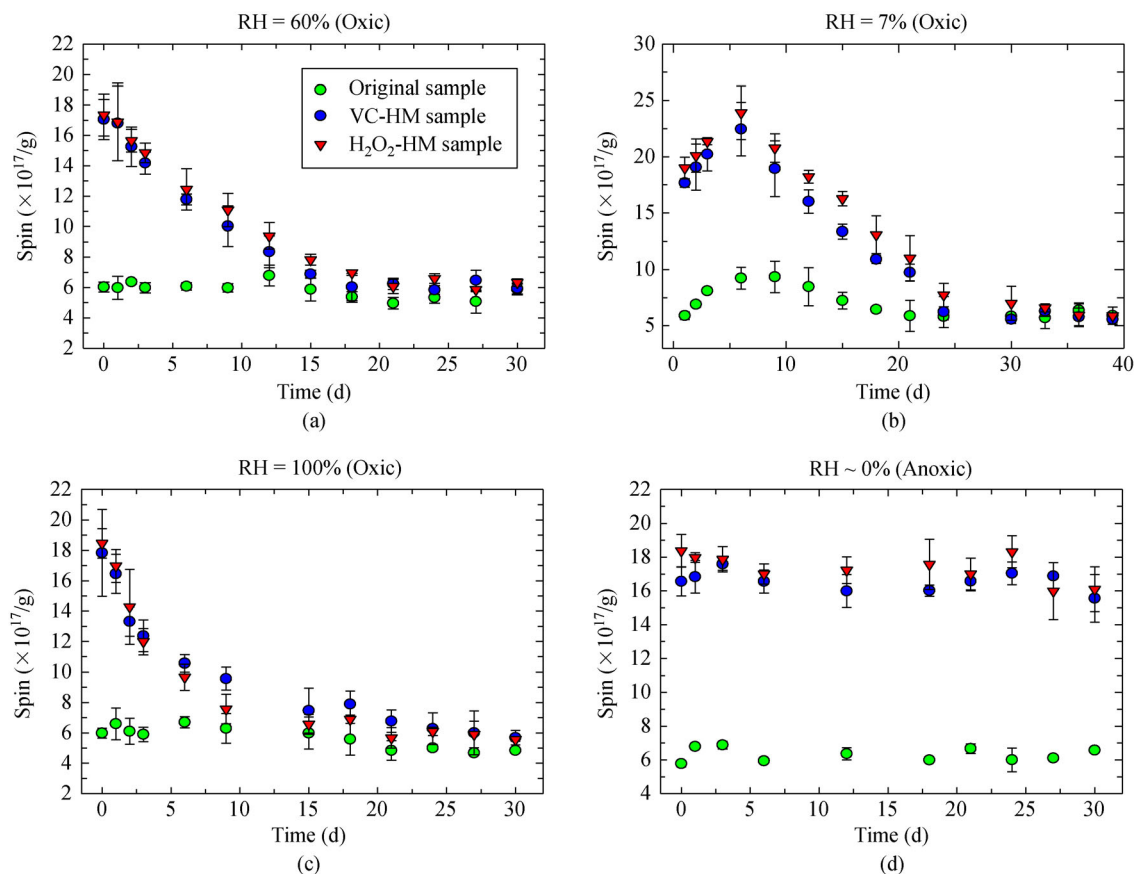
Fig. 3 Evolution of spin densities as a function of aging time for the originally isolated HM, H_2O_2- and L-ascorbic acid-treated HM samples under different conditions, such as (a) Air, RH = 60%, (b) air, RH = 7%, (c) Air, ~100%, and (d) no Air, RH = 0%.

upon exposure to air (Table S2). Further aging of HM and particulate matter samples resulted in a decrease in the spin densities of the matrix (Maskos and Dellinger, 2008).

The spin density of VC-HM increased initially, reaching the highest value of 23×10^{17} spins/g after 6 d, and then decreased gradually to a value equivalent to that of the original HM. The oxidative sample, i.e., H_2O_2-HM, also showed similar phenomena (Fig. 3(b)). The decays of PFRs were derived from the reaction time at their highest yield for H_2O_2-HM and VC-HM samples (Fig. S3b). HM-PFRs exhibited slightly longer lifetimes under dehydrated conditions compared to that associated with a RH of ~60%. Overall, the free radicals produced by the reductive/oxidative treatment of HM were unstable and readily disappeared completely under natural conditions. This may be because the redox-induced free organic radicals were mainly derived from phenolic/quinone-type moieties (Khachatryan et al., 2006). These radicals were sensitive to external paramagnetic species (possibly, oxygen molecules) (Maskos et al., 2005). As reported previously, the oxygen molecule had an influence upon relaxation properties of paramagnetic centers of the HM sample, which strongly diminished the saturation of signals (Gohre et al., 1986). Thus, the increased spin densities of HM were readily recovered to the origin state via electron transfer to

other molecules (Oniki and Takahama, 1994). Overall, air exposure of the treated HM samples involved two opposite chemical processes: formation and annihilation.

Figure 3(c) displays the evolution of spin densities of the aged HM samples under oxic conditions at RH = ~100%. The radical concentrations of the three HM samples exhibited a slightly "fast" decay with 1/e lifetimes of 10–12 d, compared to their exposure in air at RH = ~60% (Fig. S3(c)). The decay rates of radical concentrations for H_2O_2-HM or VC-HM samples were higher than that of the original sample. Exposure to water vapor not only inhibited the formation of new free organic radicals (or secondary radicals) but also quenched the generation of radicals via the following possibilities. One possibility is that water molecules were adsorbed on two hydroxyl groups and formed hydroxide groups (dissociative chemisorption) (Maskos and Dellinger, 2008), which induced the recombination of free radicals. Therefore, the increase in the concentration of water molecules enhanced the annihilation of the radicals, and the removal of water favored chemisorption and radical formation. Another possibility is the contribution of the suppression effect from the interaction between HM moieties with free radicals and water molecules (Jia et al., 2016). Oxygen atom donors such as H_2O molecules were involved in the

coordination of radical species in HS, inducing the formation of hydrogen bonds with the phenolic groups (Maskos and Dellinger, 2008). Therefore, the hydration process resulted in a significant decay of radical concentration (Fig. 3(c)). Comparatively, the aging of soil samples under anoxic conditions with almost no humidity and oxygen content resulted in relatively constant spin densities of all samples (Fig. 3(d)). During the aging period, the *g*-factors also remained in variants of ~2.0025, ~2.0042 and ~2.0038. This indicated that the free organic radicals in HM may attain stabilization under anoxic conditions without water.
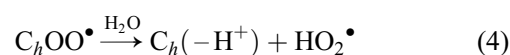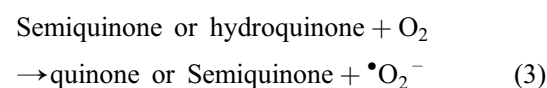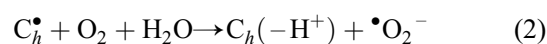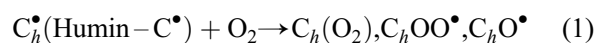
To probe the stability of PFRs, the VC-HM samples treated with various concentrations of VC were aged under oxic conditions at RH = ~60%. As shown in Fig. S4, VC-HM samples exhibited different decay rates. The spin densities of the original HM remained relatively constant during an aging period of two months. In contrast, the spin density gradually decreased with the elapsed aging time for the VC-HM samples. The VC-HM samples at high concentrations of VC had higher amounts of free radicals, which decayed rapidly. The obtained results further indicated that the newly generated free organic radicals on HM were unstable, compared to the original HM samples.
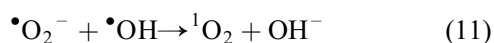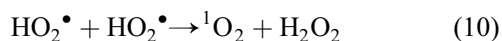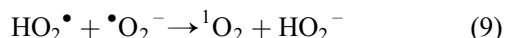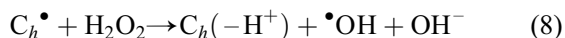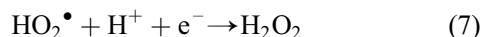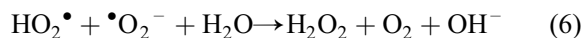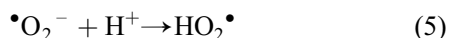
As discussed above, HM-associated free organic radicals could be classified into two types of radicals: the relatively stable ones that persisted over a long period of time, and the transient ones with relatively short life spans. This might be due to the presence of multiple redox-mediating moieties in HM; one type was stable under various conditions, whereas the other type was more susceptible to ambient conditions such as pH, chemical reduction, and irradiation (Oniki and Takahama, 1994). In the original HM sample, the detected free organic radicals mainly existed as the persistent species (Senesi et al., 1977). The observed radicals in the original sample may be from the quinhydrone-type complexes between the donors and the acceptors (Oniki and Takahama, 1994). These quinhydrone-type radicals were relatively stable under natural conditions, resulting in the EPR signal in HM (Oniki and Takahama, 1994). Additionally, we could not exclude the contribution of EPR signals from other sources such as thiyl-type radicals, nitrogen functional groups, or metal-organic complexes (Rex, 1960). Conversely, a large number of remaining electron donors (i.e., phenolic OH) and electron acceptors (i.e., quinone type moieties) in NOM are free to form the complexes due to the steric hindrance (Oniki and Takahama, 1994). Oxidation of HM promotes the generation of semiquinone-type radicals, which could produce the phenolic OH groups by one-electron oxidation. The treatment by reductive agents could be due to the quinone-type moieties by one-electron reduction. These hydroquinones were readily re-oxidized in the presence of air.

3.3 Generation of ROS

The spin-trapping EPR technique was applied to gain an understanding of the formation of ROS. As shown in Fig. S5, various types of ROS were produced on HM samples. The 4-line and 3-line EPR spectra, which were individually assigned to the characteristics of DMPO-OH (a^N = 14.3 G, $a_{\hat{a}}^H$ = 12.7 G, and $a_{\hat{a}}^H$ = 0.61 G) and DMPO-$^1O_2$ (a^N = 14.4 G and a^H = 13.5 G), were detected in DMPO aqueous solutions, suggesting the formation of $^\bullet$OH and $^1O_2$. A 6-line signal (α_N = 14.00 G, α_H^β = 9.8 G, and α_H^β = 1.40 G) in EPR spectra was detected using DMSO as the media, indicating the formation of DMPO-OOH (Fig. S6). These results supported the formation of $^\bullet$OH, $^1O_2$, and $^\bullet O_2^-$.

The generation of ROS could be attributed to the reaction of HM-EPFRs with oxygen. The exposure of newly modified-HM samples to air leads to the interaction between C-centered free radicals and oxygen to yield valence-saturated and other free radical intermediates (Eq. (1); *h* represents the HM matrix) (Radovic, 2009). The chemisorbed oxygen may be incorporated into organoperoxide, alcohol, quinone, oxyl, and semiquinone radical groups (Cwielag-Piasecka et al., 2017; Zhu et al., 2019). When the modified-HM is suspended into aqueous solution, direct electron transfer to oxygen from C-centered radical sites (Eq. (2)) or from semiquinone or hydroquinone groups (Eq. (3)) occurs to produce $^\bullet O_2^-$ (Fang et al., 2015, Zhu et al., 2017). The hydrolytic elimination of $HO_2^\bullet$ may occur via Eq. (4). Eq. (5) shows the spontaneous production of $HO_2^\bullet$. The produced $^\bullet O_2^-$ and $HO_2^\bullet$ are further transformed into H_2O_2 by their disproportionation (Eq. (6)) (Campos-Martin et al., 2006). $^\bullet O_2^- / HO_2^\bullet$ many also undergo one-electron reduction by HM to H_2O_2 (Eq. (7)). H_2O_2 may further be decomposed to $^\bullet$OH by one-electron reduction of EPFRs and the reduced quinone moieties (Eq. (8)) (Khachatryan et al., 2014; Sharma et al., 2019). In addition, the interactions between $^\bullet O_2^-$, H_2O_2, $HO_2^\bullet$, and $^\bullet$OH may induce the formation of $^1O_2$ (Eqs. (9-11)) (Wang et al., 2018). In this process, quinones in HM were crucial to promote the formation of free radicals (Khachatryan and Dellinger, 2011). Therefore, the production of ROS was most likely owing to the interactions among the free radicals, i.e., free electron on HM moieties, with small molecules, as well as the contribution of quinones in HM samples.

$$C_h^\bullet(\text{Humin} - C^\bullet) + O_2 \rightarrow C_h(O_2), C_hOO^\bullet, C_hO^\bullet \quad (1)$$

$$C_h^\bullet + O_2 + H_2O \rightarrow C_h(-H^+) + {}^\bullet O_2^- \quad (2)$$

$$\text{Semiquinone or hydroquinone} + O_2$$
$$\rightarrow \text{quinone or Semiquinone} + {}^\bullet O_2^- \quad (3)$$

$$C_hOO^\bullet \xrightarrow{H_2O} C_h(-H^+) + HO_2^\bullet \quad (4)$$

$$\bullet O_2{}^- + H^+ \rightarrow HO_2{}^\bullet \tag{5}$$

$$HO_2{}^\bullet + {}^\bullet O_2{}^- + H_2O \rightarrow H_2O_2 + O_2 + OH^- \tag{6}$$

$$HO_2{}^\bullet + H^+ + e^- \rightarrow H_2O_2 \tag{7}$$

$$C_h{}^\bullet + H_2O_2 \rightarrow C_h(-H^+) + {}^\bullet OH + OH^- \tag{8}$$

$$HO_2{}^\bullet + {}^\bullet O_2{}^- \rightarrow {}^1O_2 + HO_2{}^- \tag{9}$$

$$HO_2{}^\bullet + HO_2{}^\bullet \rightarrow {}^1O_2 + H_2O_2 \tag{10}$$

$${}^\bullet O_2{}^- + {}^\bullet OH \rightarrow {}^1O_2 + OH^- \tag{11}$$

The concentrations of ROS were quantified with the DMPO spin adduct formation. In this study, the production of ROS by the original HM sample was applied as a control experiment. As shown in Fig. S5 and Table S3, the concentrations of $\bullet OH$ and $\bullet O_2{}^-$ in original HM were undetectable. Compared to the original sample, more ROS were detected in the H_2O_2-HM or VC-HM samples. In the VC-HM sample treated by 0.08 M VC, the spin densities of $\bullet OH$ and $^1O_2$ increased to 2.32×10^{16} and 1.71×10^{16} spins/g, respectively (Table S3). The concentration of DMPO-OOH increased from 0.31×10^{16} to 0.56×10^{16} spins/g when the concentration of VC for HM treatment increased from 0.01 to 0.08 mol/L. The change in HM characteristics such as free organic radicals and other physicochemical properties during the reductive/oxidative treatments could be responsible for the difference of DMPO-ROS adducts between the treated HM sample and the original sample. It was noted that the formation of DMPO-OH was correlated with the variation of spin densities of HM. There was a positive correlation between the concentrations of ROS and EPFRs of HM (Fig. 4). The detected $\bullet O_2{}^-$ exhibited a similar trend. These results suggested that the newly produced transient/unstable radicals easily induced the formation of ROS via electron transfer. The persistent free radicals in the original HM were inactive, and rarely promoted the formation of ROS.

3.4 Transformation of PAHs

The potential transformations of PAHs on HM samples were investigated under a RH of 60% at room temperature. The reaction occurred spontaneously over a period of days, and the decay of various PAHs as a function of reaction time is shown in Fig. 5(a). It was noted that the concentration of PAHs decreased rapidly on the 9th d of reaction associated with 0.01 mol/L VC-HM, followed by a slow decay over a prolonged period. After 15 d of reaction, almost 28%, 23%, 21%, and 15% of initially spiked B[a]P, ANP, PHE, and NAP, respectively, were transformed in HM samples treated by 0.01 mol/L VC. To evaluate the possible effect of HM adsorption on the disappearance of PAHs, control experiments were con-
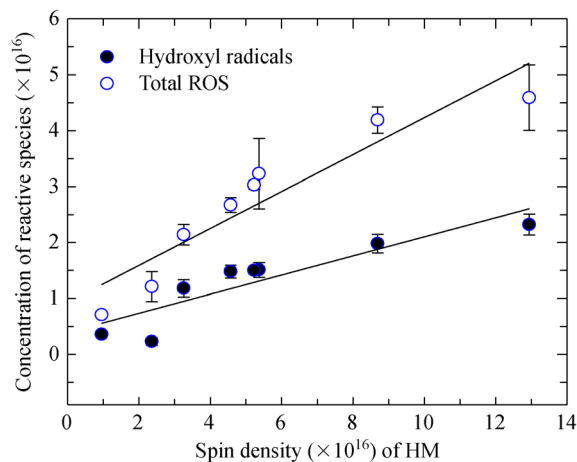

Fig. 4 Variation of concentrations of hydroxyl radials and ROS with concentration of EPFRs of HM samples treated by H_2O_2 and L-ascorbic acid.

ducted under anoxic conditions. No significant decays of these PAHs ($<5\%$) were observed in these control experiments during the studied reaction period. This observation suggested that the HM significantly promoted the transformation of PAHs. This could be due to the participation of ROS produced on the reduced HM sample. The fitting of results indicated that the transformation of PAHs followed a pseudo-first-order model in the studied reaction systems, and the normalized rate constants by carbon amounts are given in Table S4. Overall, the mediated transformation rate followed the order of B[a]P>ANT>PHE>NAP. The obtained results suggested that the HM-mediated degradation of PAHs strongly depended on their molecular properties. High-molecular-weight compounds were degraded more readily compared to PAHs with a smaller number of aromatic rings. The radical-mediated reaction preferentially attacked the "tertiary carbon atoms" of PAH molecules (Wang et al., 2019). The transformation rate was correlated to the half-wave-potential ($E_{1/2}$) of organic contaminants. PAH molecules with low $E_{1/2}$ values exhibited favorability toward oxidative transformation (Jia et al., 2018). Thus, the decay rates of B[a]P ($E_{1/2} = 0.94$) and ANT ($E_{1/2} = 1.09$) were higher than those of low-molecular-weight PAHs, such as PHE ($E_{1/2} = 1.50$) and NAP ($E_{1/2} = 1.70$) (Rechcigl and Co, 1977).

The carbon normalized transformation rate constants of ANT were 0.0732, 0.1137, 0.1748, and 0.1749 d^{-1} for VC-HM samples treated by 0.02, 0.04, 0.08, and 0.10 mol/L VC, respectively (Fig. 5(b) and Table S4). Overall, the transformation rate of ANT by VC-HM samples followed an increasing trend with increasing VC addition when its concentration was lower than 0.08 mol/L. For the HM treated by 0.08 mol/L and 0.1 mol/L VC, a similar disappearance rate was observed. Similarly, HM samples treated by H_2O_2 also promoted the degradation of ANT
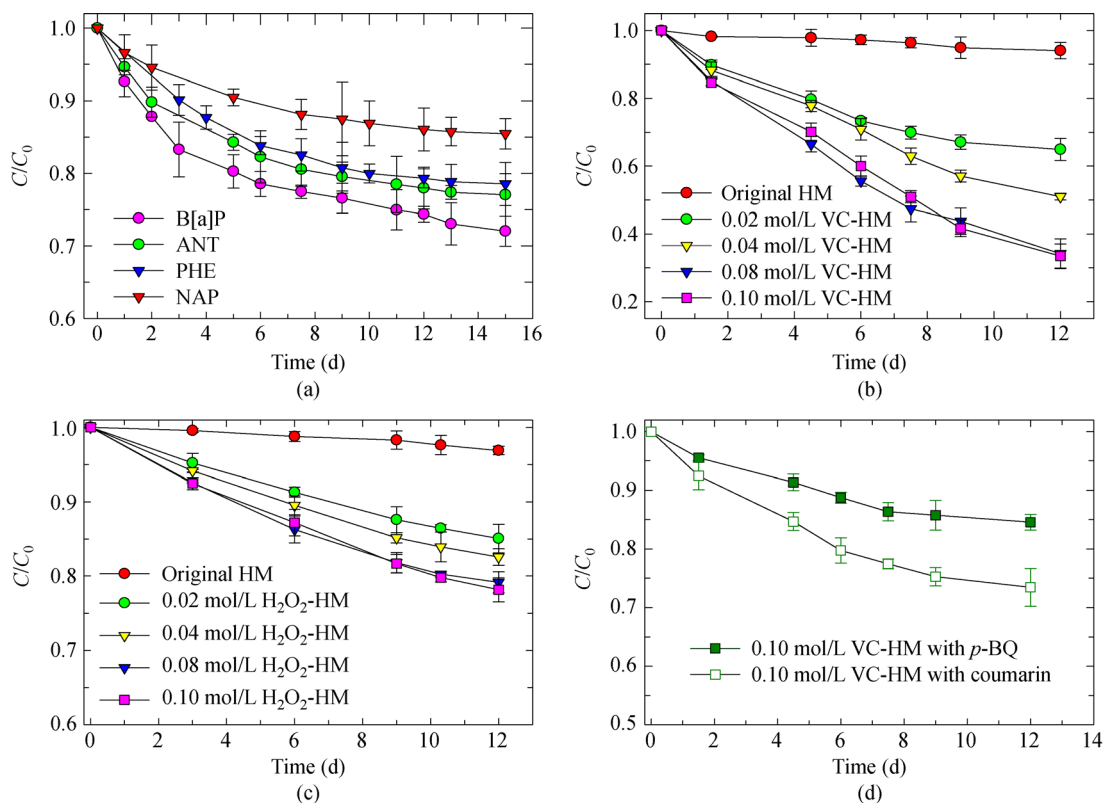
Fig. 5 (a) Evolution of PAHs, including benzo[a]pyrene (B[a]P), anthracene (ANT), phenanthrene (PHE), and naphthalene (NAP), as a function of reaction time during the transformation process by 0.10 mol/L L-ascorbic acid-HM sample; Evolution of ANT as a function of reaction time in the reaction systems involving in HM samples treated by different amounts of (b) H_2O_2 and (c) L-ascorbic acid. (d) Transformation of ANT by 0.10 mol/L L-ascorbic acid-HM in the presence of coumarin and benzoquinone.

(Fig. 5(c) and Table S4). The obtained results suggested that the transformation ability of HM on PAHs was correlated with their reductive/oxidative extent.

The oxidation ability of HM samples was consistent with their radical concentrations and potential generation of ROS. The accelerated transformation rate of ANT by VC-treated HM might be due to their enhanced production of ROS (Fig. S5). To further explore the relevant ROS contributing to ANT degradation, coumarin, p-BQ, or Na_3N were individually added into the ANT-HM system. Previous studies reported that coumarin, p-BQ, and Na_3N were effective quenching agents for $^{\bullet}OH$, $^{\bullet}O_2^-$, and $^1O_2$, respectively (Jia et al., 2015). When radical scavengers were introduced into the PAH-spiked HM samples, they would be adsorbed on HM and compete with PAHs for radical-induced reactions (Jia et al., 2015). As shown in Fig. 5(d), the existence of coumarin or p-BQ slowed down the decay of ANT; the normalized transformation rate constants of ANT on 0.10 M VC-HM decreased from 0.1749 to 0.0266 or 0.0493 d^{-1} in the presence of p-BQ or coumarin, respectively. These results suggested that both $^{\bullet}OH$ and $^{\bullet}O_2^-$ could be involved in the transformation of ANT on VC-HM. Meanwhile, $^{\bullet}O_2^-$ played a more important role in ANT transformation than that of $^{\bullet}OH$, which might be because the production of $^{\bullet}OH$ followed

the mechanism of $^{\bullet}O_2^-$ generation. The suppressing effect from other scavengers, such as Na_3N, in the transformation of ANT was negligible. Overall, ROS played a vital role in the degradation of PAHs.

4   Conclusions

This study demonstrated that solid-state metal-free HM possessed a previously unrecognized stable electron-mediating capacity, i.e., persistent free radicals, which may induce electron transfer reactions in soil. HM-associated free radicals were sensitive to variation under redox conditions. The reductive process significantly increased the amount of PFRs, indicating that water-logged or poorly-drained soils, where reducing conditions prevail, may contain high concentrations of organic free radicals. The newly produced free radicals were reversible and could be readily re-oxidized under the studied conditions. Release of electrons promoted the generation of ROS and other electron transfer reactions. The formation of ROS under dark conditions during oxidation of reduced HA represented a previously unknown source of $^{\bullet}OH$ formation at oxic/anoxic interfaces. The generated ROS may initiate the transformation of organic contami-

nants such as PAHs bonding with HM fractions in soil. Therefore, the evolution of free radicals in HM may affect the transformation dynamics and fate of contaminants under natural conditions. The results of this study may have important implications for the properties of humic-based redox-mediators and the reductants needed for their successful applications in remediation strategies/technologies. These findings also indicated that HM may be a naturally occurring solid electron acceptor/donor, which could be utilized in applications to remediate pollutants.

References

Campos-Martin J M, Blanco-Brieva G, Fierro J L G (2006). Hydrogen peroxide synthesis: An outlook beyond the anthraquinone process. Angewandte Chemie International Edition, 45(42): 6962–6984

Cwielag-Piasecka I, Witwicki M, Jerzykiewicz M, Jezierska J (2017). Can carbamates undergo radical oxidation in the soil environment? A case study on carbaryl and carbofuran. Environmental Science & Technology, 51(24): 14124–14134

Fang G, Zhu C, Dionysiou D D, Gao J, Zhou D (2015). Mechanism of hydroxyl radical generation from biochar suspensions: implications to diethyl phthalate degradation. Bioresource Technology, 176: 210–217

Gohre K, Scholl R, Miller G C (1986). Singlet oxygen reactions on irradiated soil surfaces. Environmental Science & Technology, 20(9): 934–938

Jia H Z, Li L, Chen H X, Zhao Y, Li X Y, Wang C Y (2015). Exchangeable cations-mediated photodegradation of polycyclic aromatic hydrocarbons (PAHs) on smectite surface under visible light. Journal of Hazardous Materials, 287: 16–23

Jia H Z, Nulaji G, Gao H W, Wang F, Zhu Y Q, Wang C (2016). Formation and stabilization of environmentally persistent free radicals induced by the interaction of anthracene with Fe(III)-modified clays. Environmental Science & Technology, 50(12): 6310–6319

Jia H Z, Zhao J C, Fan X Y, Dilimulati K, Wang C Y (2012). Photodegradation of phenanthrene on cation-modified clays under visible light. Applied Catalysis B: Environmental, 123-124: 43–51

Jia H Z, Zhao S, Shi Y F, Zhu L Y, Wang C Y, Sharma V K (2018). Transformation of polycyclic aromatic hydrocarbons and formation of environmentally persistent free radicals on modified montmorillonite: The role of surface metal ions and polycyclic aromatic hydrocarbon molecular properties. Environmental Science & Technology, 52(10): 5725–5733

Jin X, Kengara F O, Yue X, Wang F, Schroll R, Munch J C, Gu C, Jiang X (2019). Shorter interval and multiple flooding-drying cycling enhanced the mineralization of ^{14}C-DDT in a paddy soil. Science of the Total Environment, 676: 420–428

Khachatryan L, Adounkpe J, Maskos Z, Dellinger B (2006). Formation of cyclopentadienyl radical from the gas-phase pyrolysis of hydroquinone, catechol, and phenol. Environmental Science & Technology, 40(16): 5071–5076

Khachatryan L, Dellinger B (2011). Environmentally persistent free radicals (EPFRs)-2. Are free hydroxyl radicals generated in aqueous solutions? Environmental Science & Technology, 45(21): 9232–9239

Khachatryan L, McFerrin C A, Hall R W, Dellinger B (2014). Environmentally persistent free radicals (EPFRs). 3. Free versus bound hydroxyl radicals in EPFR aqueous solutions. Environmental Science & Technology, 48(16): 9220–9226

Li Y, Niu J, Shang E, Crittenden J C (2016). Influence of dissolved organic matter on photogenerated reactive oxygen species and metal-oxide nanoparticle toxicity. Water Research, 98: 9–18

Maskos Z, Dellinger B (2008). Formation of the secondary radicals from the aging of tobacco smoke. Energy & Fuels, 22(1): 382–388

Maskos Z, Khachatryan L, Dellinger B (2005). Precursors of radicals in tobacco smoke and the role of particulate matter in forming and stabilizing radicals. Energy & Fuels, 19(6): 2466–2473

Munk L, Sitarz A K, Kalyani D C, Mikkelsen J D, Meyer A S (2015). Can laccases catalyze bond cleavage in lignin? Biotechnology Advances, 33(1): 13–24

Oniki T, Takahama U (1994). Effects of reaction time, chemical reduction, and oxidation on ESR in aqueous solutions of humic acids. Soil Science, 158(3): 204–210

Page S E, Sander M, Arnold W A, McNeill K (2012). Hydroxyl radical formation upon oxidation of reduced humic acids by oxygen in the dark. Environmental Science & Technology, 46(3): 1590–1597

Paul A, Stosser R, Zehl A, Zwirnmann E, Vogt R D, Steinberg C E W (2006). Nature and abundance of organic radicals in natural organic matter: Effect of pH and irradiation. Environmental Science & Technology, 40(19): 5897–5903

Piccolo A, Conte P, Scheunert I, Paci M (1998). Atrazine interactions with soil humic substances of different molecular structure. Journal of Environmental Quality, 27(6): 1324–1333

Radovic L R (2009). Active sites in graphene and the mechanism of CO_2 formation in carbon oxidation. Journal of the American Chemical Society, 131(47): 17166–17175

Rechcigl M, Co C R (1977). CRC Handbook Series in Nutrition and Food- Sect. D: Nutritional Requirements. v. 1: Comparative and Qualitative Requirements. Boca Raton: CRC Press

Rex R W (1960). Electron paramagnetic resonance studies of stable free radicals in lignins and humic acids. Nature, 188(4757): 1185–1186

Roden E E, Kappler A, Bauer I, Jiang J, Paul A, Stoesser R, Konishi H, Xu H F (2010). Extracellular electron transfer through microbial reduction of solid-phase humic substances. Nature Geoscience, 3(6): 417–421

Saab S C, Martin-Neto L (2004). Studies of semiquinone free radicals by ESR in the whole soil, HA, FA and humin substances. Journal of the Brazilian Chemical Society, 15(1): 34–37

Senesi N, Chen Y, Schnitzer M (1977). The role of free radicals in the

oxidation and reduction of fulvic acid. Soil Biology & Biochemistry, 9(6): 397–403

Sharma V K, Yu X, McDonald T J, Jinadatha C, Dionysiou D D, Feng M (2019). Elimination of antibiotic resistance genes and control of horizontal transfer risk by UV-based treatment of drinking water: A mini review. Frontiers of Environmental Science & Engineering, 13 (3): 2–10

Simpson A J (2002). Determining the molecular weight, aggregation, structures and interactions of natural organic matter using diffusion ordered spectroscopy. Magnetic Resonance in Chemistry, 40(13): S72–S82

Tian Y J, Zou J R, Feng L, Zhang L Q, Liu Y Z (2019). Chlorella vulgaris enhance the photodegradation of chlortetracycline in aqueous solution via extracellular organic matters (EOMs): Role of triplet state EOMs. Water Research, 149: 35–41

Vejerano E P, Rao G Y, Khachatryan L, Cormier S A, Lomnicki S (2018). Environmentally persistent free radicals: insights on a new class of pollutants. Environmental Science & Technology, 52(5): 2468–2481

Wang C, Li Y Z, Tan H, Zhang A K, Xie Y L, Wu B, Xu H (2019). A novel microbe consortium, nano-visible light photocatalyst and microcapsule system to degrade PAHs. Chemical Engineering Journal, 359: 1065–1074

Wang T C, Cao Y, Qu G Z, Sun Q H, Xia T J, Guo X T, Jia H Z, Zhu L Y (2018). Novel Cu(II)EDTA decomplexation by discharge plasma oxidation and coupled Cu removal by alkaline precipitation: Underneath mechanisms. Environmental Science & Technology, 52 (14): 7884–7891

Zhang K K, Sun P, Zhang Y R (2019). Decontamination of Cr(VI) facilitated formation of persistent free radicals on rice husk derived biochar. Frontiers of Environmental Science & Engineering, 13(2): 85–93

Zhu K C, Jia H Z, Zhao S, Xia T J, Guo X T, Wang T C, Zhu L Y (2019). Formation of environmentally persistent free radicals on micro-plastics under light irradiation. Environmental Science & Technology, 53(14): 8177–8186

Zhu K, Jia H, Wang F, Zhu Y, Wang C, Ma C(2017). Efficient removal of Pb(II) from aqueous solution by modified montmorillonite/carbon composite: Equilibrium, Kinetics and Thermodynamics. Journal of Chemical & Engineering Data, 62(1): 333–340